© 1998 Oxford University Press
Nucleic Acids Research, 1998, Vol. 26, No. 5 **1345–1351**

Crystal structures of MS2 coat protein mutants in complex with wild-type RNA operator fragments

Sjoerd H. E. van den Worm[+], Nicola J. Stonehouse[1], Karin Valegård, James B. Murray[1], Catherine Walton[1], Kerstin Fridborg, Peter G. Stockley[1] and Lars Liljas*

Department of Molecular Biology, Uppsala University, Box 590, S-751 24 Uppsala, Sweden and
[1]Department of Biology, University of Leeds, Leeds LS2 9JT, UK

Received September 30, 1997; Revised and Accepted January 14, 1998

PDB nos 1mva, 1mvb, 1aq4, 1aq3

ABSTRACT

In MS2 assembly of phage particles results from an interaction between a coat protein dimer and a stem–loop of the RNA genome (the operator hairpin). Amino acid residues Thr45, which is universally conserved among the small RNA phages, and Thr59 are part of the specific RNA binding pocket and interact directly with the RNA; the former through a hydrogen bond, the latter through hydrophobic contacts. The crystal structures of MS2 protein capsids formed by mutants Thr45Ala and Thr59Ser, both with and without the 19 nt wild-type operator hairpin bound, are reported here. The RNA hairpin binds to these mutants in a similar way to its binding to wild-type protein. In a companion paper both mutants are shown to be deficient in RNA binding in an *in vivo* assay, but *in vitro* the equilibrium dissociation constant is significantly higher than wild-type for the Thr45Ala mutant. The change in binding affinity of the Thr45Ala mutant is probably a direct consequence of removal of direct hydrogen bonds between the protein and the RNA. The properties of the Thr59Ser mutant are more difficult to explain, but are consistent with a loss of non-polar contact.

INTRODUCTION

MS2 is a group I RNA bacteriophage which infects *Escherichia coli* (1). Other related viruses are GA, Qβ and SP, which belong to groups 2, 3 and 4 respectively. The icosahedral shell of MS2 virus particles is made up of 180 copies of the coat protein subunit arranged as a $T = 3$ quasi-equivalent surface lattice, which packages a plus sense RNA of 3569 nt. The quasi-equivalent coat protein conformers, known as A, B and C, pack as non-covalent A/B and C/C dimers in the capsid (2). The genomic RNA encodes four proteins: the maturation protein, the coat protein subunit, a replicase subunit and the lysis protein.

In solution MS2 coat protein exists as a dimer, which has a dual function: it is the basic building block of the capsid and it acts as a translational repressor of the replicase gene. This latter function is accomplished by a sequence-specific RNA–protein interaction, in which a coat protein dimer binds to an RNA stem–loop structure, called the operator hairpin, which bears the Shine–Dalgarno (SD) sequence and the start codon of the replicase gene (Fig. 1). This specific recognition is also responsible for the specificity of RNA encapsidation and acts as a catalyst for capsid assembly.

Recently the crystal structure of the viral capsid with the 19 nt operator hairpin bound was solved (3,4). This was achieved by soaking crystals of recombinant capsids (which lack the genomic RNA) with operator RNA. We showed that a single operator hairpin was bound in an asymmetrical fashion to the A/B quasi-two-fold dimer. The hairpin also binds to the symmetrical C/C dimer. This, however, results in superimposition of the electron density for two RNA molecules related by the two-fold axis, making interpretation more difficult. In the RNA–protein complex the adenines at positions –4 and –10 (see Fig. 1 for numbering scheme) occupied quasi-equivalent pockets formed by residues Val29, Thr45, Ser47, Thr59 and Lys61, of which only Thr59 is not evolutionarily conserved. Val29, Thr59 and Lys61 line the walls of the pocket, whereas Thr45 and Ser47 make specific but different contacts with the nucleotides in each pocket.

To date, crystal structures are known for very few specific protein–RNA complexes (5). These include a number of complexes between tRNA and aminoacyl-tRNA synthetases (6) and the structure of an RNA hairpin bound to the U1A protein from the U1 snRNP splicing complex (7). In the case of the U1A snRNA complex RNA affinities of mutant proteins have been studied (8), but structure determinations of these protein mutants or variants of the RNA have not been reported.

The aim of the present work was to study protein–RNA interactions in MS2 coat protein–RNA complexes where important residues in the protein have been mutated, to determine what effects these changes have, if any, on the conformation of the molecules and to correlate the structural results with biochemical studies. We have chosen to study two mutants, Thr45Ala and Thr59Ser. The first was selected to examine the effect of deleting the direct interaction of the side chain of Thr45 with the RNA; the importance of this residue can be judged by the universal conservation of this residue among related phages. The importance

*To whom correspondance should be addressed. Tel: +46 18 471 4204; Fax: +46 18 536 971; Email: lars@xray.bmc.uu.se

[+]Present address: Leiden Institute of Chemistry, Gorlaeus Laboratories, Leiden University, PO Box 9502, NL-2300 RA Leiden, The Netherlands

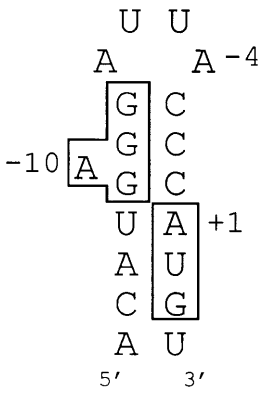

Figure 1. Secondary structure of the 19 nt operator fragment at the start of the replicase gene. The Shine–Dalgarno sequence and start codon are boxed.

for RNA binding of Thr59 is unclear, since the side chain has only limited contact with the RNA and it can apparently be substituted by glutamine in the coat proteins of phages of groups 3 and 4 (9). The Thr59Ser mutant was isolated earlier by screening for mutants deficient in repression of replicase synthesis (10,11). In the accompanying paper (12) both the Thr45Ala and the Thr59Ser mutants are shown to be unable to prevent phage infection in an *in vivo* repression assay, but only Thr45Ala has a significantly higher equilibrium dissociation constant *in vitro* than the wild-type protein. In this work we report the crystal structures of capsids of both these mutants and of complexes with the wild-type operator hairpin. Despite the deleted contacts, the RNA hairpin binds to the proteins and both resulting complexes are similar to wild-type (3,4).

MATERIALS AND METHODS

The mutants Thr45Ala and Thr59Ser were constructed, expressed and purified as described previously (13–15). Further purification and crystallization of the 'empty' capsids were achieved as described by Valegård *et al.* (16). The crystals obtained were isomorphous with the wild-type. The space group is R32; cell dimensions are $a = b = 288$ Å, $c = 653$ Å. RNA was synthesized as described by Murray *et al.* (17). Capsid crystals were washed in a buffer containing 0.4 M sodium phosphate, pH 7.4, 5% (w/v) PEG8000, 0.1 mM dithiothreitol and Promega RNasin inhibitor at 1 U/ml. RNA (in water) was added to the crystals to a final concentration of ~2 mg/ml. Diffraction data were collected at station 9.6 at the CLRC Synchrotron in Daresbury, UK, using a MAR Research image plate detector. The oscillation angle was 0.5°. The HKL (18) and the CCP4 (19) packages were used to process the images and scale the data respectively. Table 1 shows the number and percentage of observed reflections and the scaling *R* factors.

Initial phases were taken from wild-type MS2 structures with and without bound RNA. Phase refinement by non-crystallographic symmetry averaging was carried out using the program package RAVE (20). The final electron density map was clear except for a few disordered protein side chains and the lower end of the RNA stem. The first base pair (A –15·U +4) and nucleotide C –14 were not visible and the electron densities for nucleotides –13, +2 and +3 were weak, especially in the region of the riboses. This is similar to the situation in the wild-type complex (4). Several cycles of model rebuilding using the program O (21) and crystallographic refinement using the conjugate gradient method and the program X-PLOR (22) were applied to optimize the structures. Energy parameters for RNA were modified to allow for simultaneous refinement of 2′-*endo* and 3′-*endo* sugar pucker in X-PLOR (4). Table 2 lists the *R* factors after positional and *B* factor refinement as well as the r.m.s. deviation from the ideal values of bond lengths and bond angles. An occupancy of 0.7 was used for the RNA in both complexes. This value was chosen to give temperature factors similar to those in the wild-type complex and is slightly lower than the value (0.9) used in that case.

Table 1. Number and percentage of reflections and scaling *R* factor

	T45A	T45A*RNA	T59S	T59S*RNA
Resolution (Å)	3.0	3.0	3.0	2.8
R factor	9.3 (18.2)[a]	12.8 (26.3)	9.2 (23.3)	14.6 (21.7)
Number of reflections	179377 (31098)	190898 (14247)	128511 (8748)	159163 (4585)
Degree of completeness (%)	88.7 (85.2)	92.3 (95.1)	61.8 (58.3)	63.2 (25.1)
Multiplicity	1.7 (1.8)	3.3 (3.7)	2.0 (1.9)	1.8 (1.1)

[a]Values concerning the highest resolution bin (3.2–3.0 Å for the first, 3.08–3.0 Å for the next two and 2.87–2.80 Å for the last structure) are in parentheses.

Table 2. *R* factor and deviations from ideality after refinement

	Resolution (Å)	*R* factor[a]	*R* factor[b]	r.m.s. bond length (Å)	r.m.s. bond angle (°)
T45A	10.0–3.0	23.7	19.4	0.017	1.9
T45A*RNA	10.0–3.0	25.1	19.7	0.019	1.9
T59S	10.0–3.0	21.8	17.3	0.016	2.0
T59S*RNA	10.0–2.8	25.3	20.4	0.017	1.8

[a]After positional refinement.
[b]After *B* factor refinement.

RESULTS AND DISCUSSION

Quality of the models

Four models were studied in this work: Thr45Ala and Thr59Ser protein capsids both with and without the 19 nt wild-type operator fragment bound. The RNA complexes will be referred to as Thr45Ala*RNA and Thr59Ser*RNA respectively. All four models include all of the three coat protein subunits (A, B and C) and ~200 water molecules. In the model of Thr45Ala*RNA nucleotides –13 to +3 could be included at the A/B dimer and nucleotides –13 to +1 at the C/C dimer. In the model of Thr59Ser*RNA the equivalent nucleotides were –13 to +3 and –12 to –1 respectively. The qualities of the models of the proteins were assessed with the program Procheck (23). Only one residue, SerB2 in Thr45Ala, is found in the disallowed region of the Ramachandran plot. The quality of the RNA was checked by calculating dihedral angles α to ζ and χ and the pseudorotation phase angle *P* for all residues. Comparison with the angles of yeast $tRNA^{Phe}$ (24) revealed that only the 3′-terminal residue of the model (G +3) has an unusual conformation in both complexes. This may be due to difficulties in interpreting the relatively weak density.

Capsid structure

MS2 coat protein (Fig. 2a) forms a five stranded anti-parallel β-sheet (strands βC–βG) facing the interior of the phage particle, with an N-terminal hairpin (β-sheet strands βA and βB) and two α-helices (αA and αB) shielding most of the upper surface of the β-sheet from the environment (2,25). Upon dimerization extensive contacts are formed between the subunits so that the β-sheet becomes extended to form a continuous 10 stranded sheet. The α-helices of one subunit are sandwiched between the α-helices and the N-terminal hairpin of the other subunit.

The two types of coat protein dimers in the capsid (A/B and C/C) are very similar, with the exception of the FG loops that connect β-strands F and G (Fig. 2a). The FG loops of the B subunits are bent back towards the body of the dimer and form short channels around the five-fold axes of the particle. The corresponding segments of the chain in the A and C subunits are extended and three FG loops from each of these subunits are grouped around the quasi-six-fold axis.

The conformation of the mutant proteins in the capsids with and without bound RNA is largely similar to the corresponding wild-type structures. Superimposition using the program O (26) of the wild-type structures and the structures of the mutants showed that the r.m.s. differences for all Cα atoms in all comparisons are ~0.1 Å. Some small but significant deviations are found in the proximity of the mutated residues. In Thr45Ala the side chain of Glu31 has moved slightly towards the space occupied by the methyl group of the threonine in the wild-type and Arg38, which forms a salt link with the glutamic acid, has moved in the same direction. There are also some changes in partly disordered side chains, like Asn87 and Lys43. The changes in Thr59Ser are very small. The most significant change is a slight movement of Glu89 towards Ser59.

RNA structure

Coat protein dimers have two-fold symmetry, but a single RNA fragment binds asymmetrically to a dimer, interacting with both subunits. In the capsid two orientations of the RNA are possible, but at the A/B dimer the bent FG loop of the B subunit appears to prevent the RNA binding in one of these orientations (4). The symmetrical nature of the C/C dimer means that the RNA can bind in two orientations. The map shows both orientations of the RNA superimposed, making it difficult to interpret the electron density, especially the weak density at the bottom of the stem. In the following protein–RNA interactions at the A/B dimer are discussed, since the quality of the electron density is higher and therefore can be interpreted unambiguously. In the upper region of the stem–loop structure interactions between RNA and protein are similar at the A/B and C/C dimers.

The RNA stem has an A-type helical structure (Fig. 2b) as judged by sugar puckering, inclination and twist. Three of the four nucleotides in the loop are ordered in the crystal structure, whereas the loop appears to be very flexible in solution (27). Two of the loop nucleotides are involved in base-specific RNA–protein interactions. A –4 is inserted in the RNA binding pocket of the A subunit and forms hydrophobic interactions and four hydrogen bonds (Fig. 3a and b). U –5 is not only stacked against TyrA85, but also forms hydrogen bonds with residues GluA63, TyrA85 and AsnA87 (Fig. 3c). The third important base-specific interaction is formed between A –10 and the B subunit. The NMR solution structure suggests that A –10 is predominantly intercalated in the helical stem. In the crystal structure, however, A –10 is bulged out of the stem and interacts with the RNA binding pocket on the B subunit. These interactions differ from those in the A subunit, since the adenine base is inserted in the pocket in a different orientation (Fig. 3d and e). ThrB45 makes contacts with N1 and N6 of the base, but the latter hydrogen bond is probably weak, since the relative positions of the atoms are unfavourable.

In addition to the interactions involving the bases, a number of residues (LysA43, ArgA49, GluA63, TyrA85, ArgB49, SerB52, AsnB55, LysB57 and LysB61) in the dimer are involved in direct interactions with the RNA backbone.

Thr45Ala

The Thr45Ala–operator RNA complex shows some significant differences when compared with the interactions made by wild-type. Differences occur in both A and B subunits. The hydrogen bond that is normally formed between ThrB45 Oγ1 and A –10 N1 is not present due to substitution with alanine (Fig. 3e). This loss allows the base of A –10 to move towards SerB47, albeit only by 0.2 Å. The substitution also causes a number of other small changes in the RNA and the protein in this region. The most significant change is that phosphate G –11 has moved away from the protein and the distance between O2P –11 and the side chain of LysB61 has increased by 0.5 Å, indicating a weaker link. The contact of LysB61 with A –10 O2P becomes shorter (Fig. 4).

In the A subunit movement of A –4 is more pronounced than for A –10 in the B subunit. The lost contacts at A –4 N6 and N7 do not cause the base to move towards SerA47, but sideways by 0.2 Å, out of the binding pocket (Fig. 3b). To accommodate the shift of the base all nucleotides from –2 to –5 are moved towards the major groove and away from the stem compared with the wild-type (Fig. 5). Movement of the sugar at –5 increases the distance (from 3.0 to 3.2 Å) between O2′ and GluA63 Oε2 and decreases the angle between U –5 O2′, GluA63 Oε2 and Cδ (from 107 to 92°), making this bond less favourable. As a result of the movement of LysA43, the conformation of GluA63 adapts slightly to sustain the contact

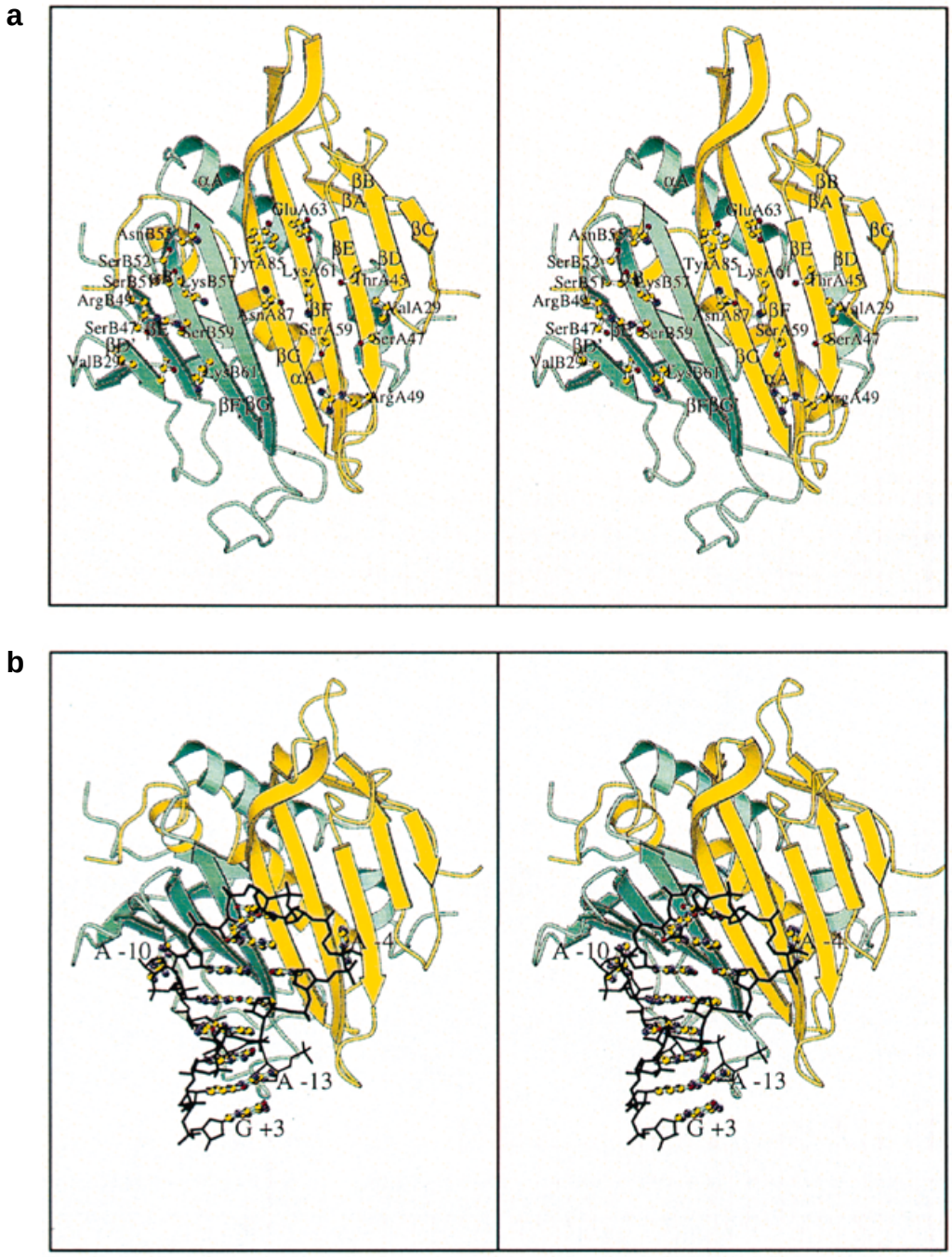

Figure 2. (**a**) Stereo drawing showing an AB′ dimer from the T59*RNA complex. The A and B′ subunits are shown in yellow and green respectively. Secondary structure elements are labelled. Note the difference in the conformation of the FG loops. All side chains in direct contact with the RNA hairpin are shown. (**b**) Stereo drawing of the wild-type operator fragment and the AB′ coat protein dimer from the T59*RNA complex. The RNA backbone is shown as bonds and the bases as balls and sticks. The model is rotated 25° around a horizontal axis compared with the view in (a). These drawings, together with Figures 3–5, are produced with the program Molscript (32).

with this residue, contributing to the loss of the hydrogen bond between GluA63 Oε2 and U –5 O2′. The hydrogen bond between U –5 O2 and AsnA87 Nδ2 becomes shorter (from 3.0 to 2.8 Å).

We conclude that the loss of five hydrogen bonds (ThrA45 Oγ1 to A –4 N6 and N7; GluA63 Oε2 to U –5 O2′; ThrB45 Oγ1 to A –10 N1 and N6) and the weakening of a salt link (LysB61 Nζ to G –11 O2P) probably leads to an overall decrease in affinity of the RNA for the protein despite some slightly strengthened contacts (AsnA87 Nδ2 to U –5 O2; LysB61 Nζ to A –10 O2P). This is consistent with the sequence conservation data for this residue and the functional data on this mutant (12).

Thr59Ser

The complex of the Thr59Ser mutant with RNA shows fewer differences from wild-type than Thr45Ala. Loss of some of the

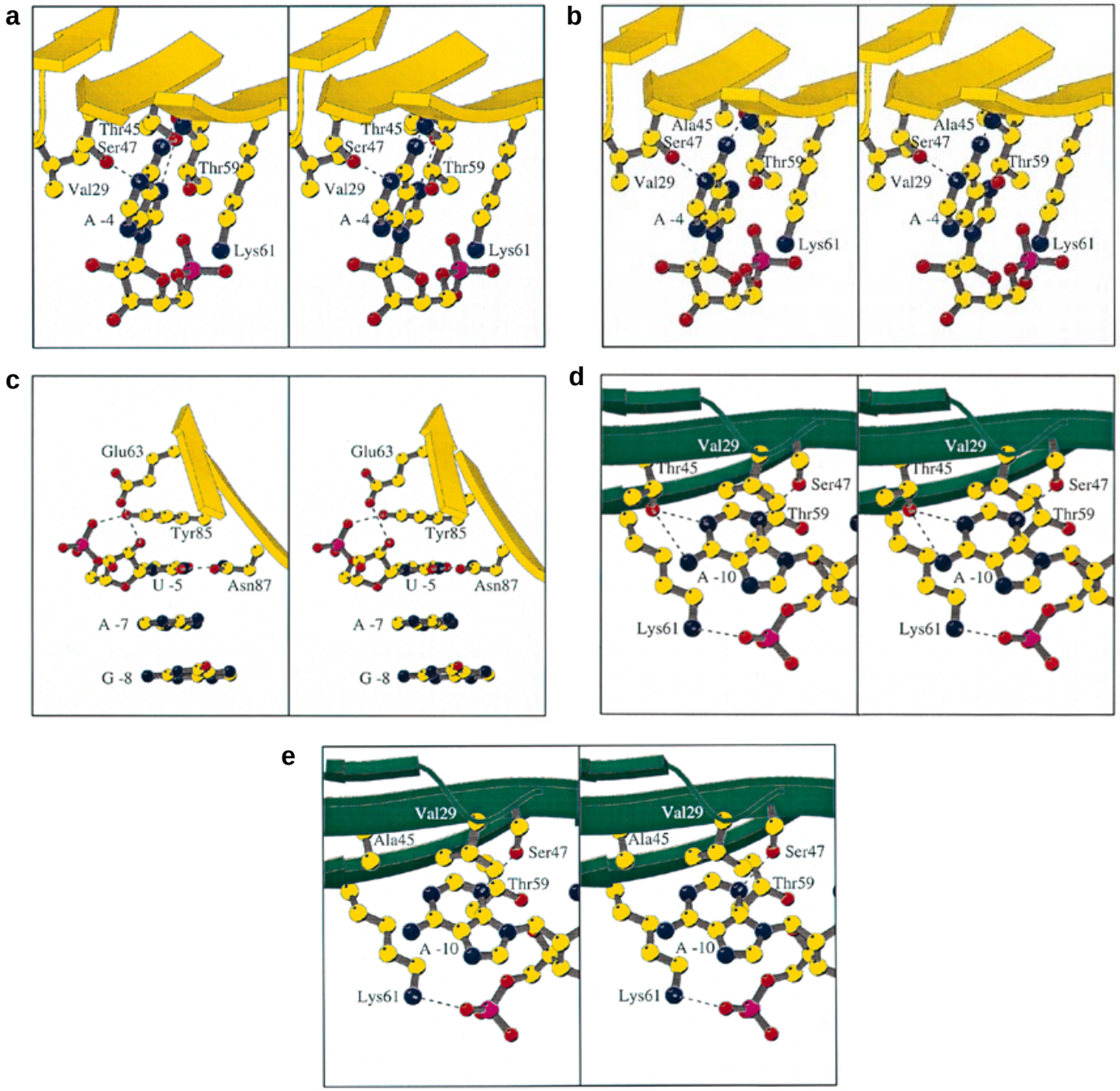

Figure 3. Stereo drawings showing details of the RNA–protein interactions in the complexes. β-Strands of the protein are shown as arrows. (**a**) Binding of A –4 to the A subunit in the wild-type complex. (**b**) Corresponding view of the T45A*RNA complex. (**c**) Binding of U –5 in the wild-type complex. (**d**) Binding of A –10 to the B subunit in the wild-type complex. (**e**) Corresponding view of the T45A*RNA complex.

hydrophobic interactions between the protein and RNA may, however, be significant. Thr59 and Lys61 form one of the walls of the pockets binding A –4 and A –10. In the wild-type complex the methyl group of Thr59 in the A subunit is packed against N1 of A –4 and in the B subunit against N3 of A –10. In this complex the change in accessible surface area due to this interaction is only ~3% (of the 700 Å^2 surface of the protein which interacts with the RNA, 25 Å^2 is contributed by the methyl groups of Thr59). It is still likely that removing this contact will decrease the stability of the complex to some extent. The positions of the bases of A –4 and A –10 are essentially the same (<0.3 Å differences).

A significant difference that is observed in the model is a shift in the side chain of Glu89 towards Ser59, probably caused by the absence of the methyl group, which is turned towards Glu89 in the wild-type structure. These shifts are 1 and 0.6 Å in the A and B subunits respectively.

In addition to the differences which lead to significant changes in the coordinates of the model, there are further differences

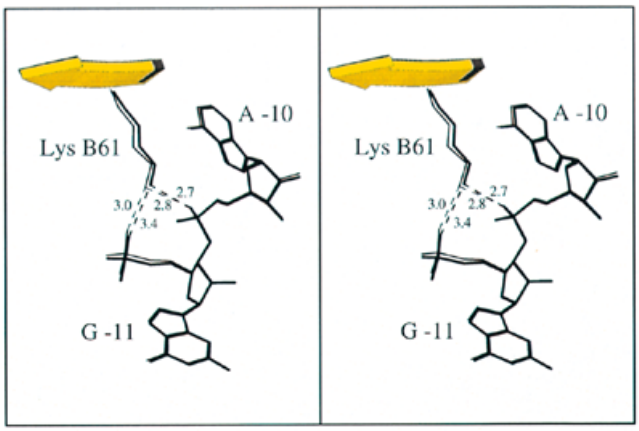

Figure 4. Stereo view of the contacts between LysB61 and the phosphates of G –11 and A –10 in the wild-type complex (thin lines) and the T45A*RNA complex (thick lines). Due to the mutation Thr45Ala, LysB61 moves away from the phosphate of G –11, thereby weakening this contact. Distances are shown in Ångstroms.

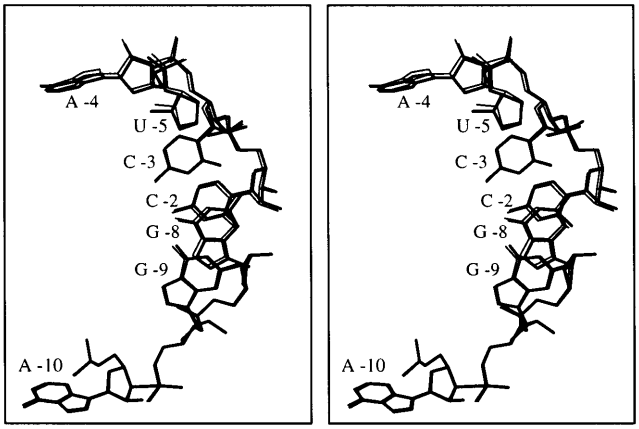

Figure 5. Stereo view of the shift of nucleotides –2 to –5 in the wild-type complex (thin lines) and the T45A*RNA complex (thick lines). The missing hydrogen bond between A –4 and residue Ala45 in the mutant Thr45Ala leads to a shift of the base and three other nucleotides move to accommodate this shift.

which can be observed in the electron density map. In the wild-type and Thr59Ser particles without RNA the side chain of GluB89 seems well ordered and interacts with LysB57. In the RNA complexes LysB57 has moved away from GluB89 and this side chain instead interacts with ArgB49 and Ser/ThrB59. The density of the GluB89 side chain is broad, however, and shows evidence of both conformations for the side chain. Close to GluB89 another difference between wild-type and Thr59Ser is observed, namely density which could be assigned to a water molecule in the wild-type complex but which is absent in the mutant (Fig. 6). This water, if present, could provide a link between GluB89 and the N6 and N7 positions of A –7. The density is weak, however, and the distances long (>3.1 Å). This bond would probably be insufficient to fix the side chain of GluB89 in one orientation, but the small shift of the side chain of GluB89 (0.6 Å) caused by the Thr59Ser mutation could be enough to disable its formation.

Conclusions

RNA–protein interaction is a dynamic process, of which we see only the end points in the complexes described here. Phenotypes for protein mutants may be caused by modifications of transient interactions or of conformational changes in the binding pathway, which would not easily be explained by the crystal structures of the final complexes. In the MS2 system the effects of mutants which cause an impaired repressor activity (10,12,28) or a lower affinity for the operator hairpin (10–12,29) can in some cases be explained by the loss of a direct polar contact (Thr45Ala, Ser47Lys, Arg49Ser, Asn87Ser or Tyr85Phe) or the introduction of a negative charge in a side chain interacting with a phosphate (Asn55Asp and Lys57Glu). In other examples (Ser47Lys and Thr91Ile) the mutant side chains are larger and would not allow binding of the RNA without conformational changes of the protein and/or the RNA.

The effects on RNA binding affinity of Thr45Ala are probably mainly explained by the missing hydrogen bonds between this

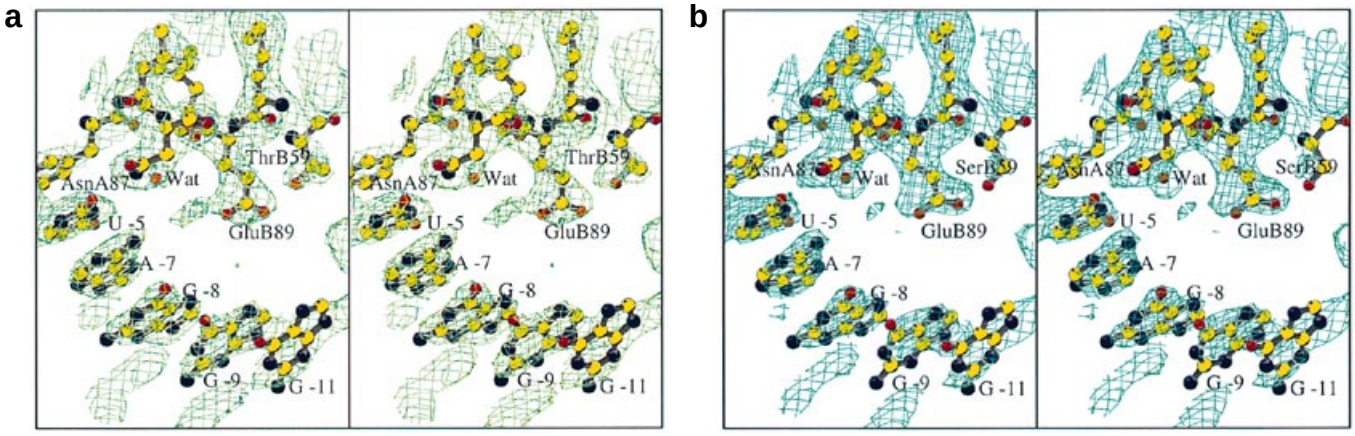

Figure 6. Stereo view of the electron density around residue GluB89 in (**a**) the wild-type complex and (**b**) the T59S*RNA complex. In the wild-type complex extra density connected to the density of GluB89 is observed. This density is absent in T59S*RNA, probably due the shift of GluB89, which is moved towards SerB59. The weak density could be assigned to a water molecule. These drawings were made using the program Bobscript, an extension of Molscript by R.Esnouf.

residue and the RNA, but might also to some extent be due to secondary changes in the complex.

The properties of the Thr59Ser mutant are more difficult to explain. The contact area between the methyl group of the threonine and the adenine base of A –4 and A –10 is small, consistent with the small increase in dissociation constant between the wild-type and the mutant (12). The fact that both the Thr59Ser and Thr59Ala mutations have an effect on RNA binding (10–12,30) while a Thr59Gln mutant, where the packing interaction might be retained, seems to have normal repressor activity (31) supports the hypothesis that loss of this contact is important for the observed phenotype. The slight decrease in affinity might be due to a hydrophobic effect related to the difference in accessible surface hidden in the complexes. A further possibility is an entropic effect: the serine of the mutant might be more flexible than the wild-type threonine in the absence of RNA and the binding of the adenine base restricts the flexibility of the serine more than it does the threonine in the respective complexes. Although it is difficult to compare the absolute values of the temperature factors, there seems to be a reduction in the flexibility of SerB59 in the RNA complex, while there is no evidence from the temperature factors of a reduction in the flexibility of ThrB59 in the wild-type complex (data not shown).

There is a possibility that the Thr59Ser mutation in addition interferes with transient interactions in the RNA binding pathway. The most significant change in the mutant seems to be the slight movement of GluB89 and possibly the loss of a water molecule bound to this side chain. The side chain of GluB89 is within 6.5 Å of A –7, G –8 and G –9 and might interact directly or indirectly with these bases in the binding pathway. The complementation studies by Peabody and Lim (28), where different mutations have been made in either one of the two 'monomers' in a genetically engineered covalently linked dimer, showed that the Thr59Ser mutant could be complemented with mutations like Tyr85His or Asn87Ser in the other 'monomer' and still retain repressor activity. Since the latter two mutants involve residues which in our complexes interact with RNA only in the A subunit, this result indicates that the effect of the Thr59Ser mutation is indeed in the B subunit.

ACKNOWLEDGEMENTS

This work was supported by the Swedish National Science Research Council, the UK BBSRC, the Leverhulme Trust and the Wellcome Trust. We thank Stephanie Fonseca and Kerstin Fridborg for technical assistance and Hugo Lago and Johan Åqvist for helpful comments. We are also grateful to David Peabody for information about unpublished results.

REFERENCES

1 Fiers,W. (1979) In Fraenkel-Conrat,H. and Wagner,R.R. (eds), *Comprehensive Virology*. Plenum, New York, NY, pp. 69–204.
2 Valegård,K., Liljas,L., Fridborg,K. and Unge,T. (1990) *Nature*, **345**, 36–41.
3 Valegård,K., Murray,J.B., Stockley,P.G., Stonehouse,N.J. and Liljas,L. (1994) *Nature*, **371**, 623–626.
4 Valegård,K., Murray,J.B., Stonehouse,N.J., van den Worm,S., Stockley,P.G. and Liljas,L. (1997) *J. Mol. Biol.*, **270**, 724–738.
5 Nagai,K. (1996) *Curr. Opin. Struct. Biol.*, **6**, 53–61.
6 Cavarelli,J. and Moras,D. (1993) *FASEB J.*, **7**, 79–86.
7 Oubridge,C., Ito,N., Evans,P.R., Teo,C.-H. and Nagai,K. (1994) *Nature*, **372**, 432–438.
8 Jessen,T.-H., Oubridge,C., Teo,C.-H., Pritchard,C. and Nagai,K. (1991) *EMBO J.*, **10**, 3447–3456.
9 Tars,K., Bundule,M., Fridborg,K. and Liljas,L. (1997) *J. Mol. Biol.*, **271**, 759–773.
10 Peabody,D.S. (1993) *EMBO J.*, **12**, 595–600.
11 Stockley,P.G., Stonehouse,N.J., Walton,C., Walters,D.A., Medina,G., Macedo,M.B., Hill,H.R., Goodman,S.T.S., Talbot,S.J., Tewary,H.K., Golmohammadi,R., Liljas,L. and Valegård,K. (1993) *Biochem. Soc. Trans.*, **21**, 627–633.
12 Lago,H., Fonseca,S.A., Murray,J.B., Stonehouse,N.J. and Stockley,P.G. (1998) *Nucleic Acids Res.*, **26**, 1337–1344.
13 Walton,C., Booth,R.K. and Stockley,P.G. (1991) In McPherson,M.J. (ed.), *Directed Mutagenesis: A Practical Approach*. IRL press, Oxford, UK, pp. 135–162.
14 Stonehouse,N.J. and Stockley,P.G. (1993) *FEBS Lett.*, **334**, 355–359.
15 Mastico,R.A., Talbot,S.J. and Stockley,P.G. (1993) *J. Gen. Virol.*, **74**, 541–548.
16 Valegård,K., Unge,T., Montelius,I., Strandberg,B. and Fiers,W. (1986) *J. Mol. Biol.*, **190**, 587–591.
17 Murray,J.B., Collier,A.K. and Arnold,J.R.P. (1994) *Anal. Biochem.*, **218**, 177–184.
18 Otwinowski,Z. and Minor,W. (1997) *Methods Enzymol.*, **276A**, 307–326.
19 Collaborative Computational Project No. 4 (1994) *Acta Crystallogr.*, **D50**, 760–763.
20 Kleywegt,G.J. and Jones,T.A. (1994) In Bailey,S., Hubbard,R. and Waller,D. (eds), *From First Map to Final Model. Proceedings of the CCP4 Study Weekend*. SERC Daresbury Laboratory, Daresbury, UK, pp. 59–66.
21 Jones,T.A., Zou,J.-Y., Cowan,S.W. and Kjeldgaard,M. (1991) *Acta Crystallogr.*, **A47**, 110–119.
22 Brünger,A.T. (1990) *XPLOR Manual*. Yale University, New Haven, CT.
23 Laskowski,R.A., MacArthur,M.W., Moss,D.S. and Thornton,J.M. (1993) *J. Appl. Crystallogr.*, **26**, 283–291.
24 Holbrook,S.R., Sussman,J.L., Warrant,R.W. and Kim,S.-H. (1978) *J. Mol. Biol.*, **123**, 631–660.
25 Golmohammadi,R., Valegård,K., Fridborg,K. and Liljas,L. (1993) *J. Mol. Biol.*, **234**, 620–639.
26 Jones,T.A., Bergdoll,M. and Kjeldgaard,M. (1990) In Bugg,C. and Ealick,S. (eds), *Crystallographic and Modeling Methods in Molecular Design*. Springer-Verlag, New York, NY, pp 189–199.
27 Borer,P.N., Lin,Y., Wang,S., Roggenbuck,M.W., Gott,J.M., Uhlenbeck,O.C. and Pelczer,I. (1995) *Biochemistry*, **34**, 6488–6503.
28 Peabody,D.S. and Lim,F. (1996) *Nucleic Acids Res.*, **24**, 2352–2359.
29 LeCuyer,K.A., Behlen,L.S. and Uhlenbeck,O.C. (1996) *EMBO J.*, **15**, 6847–6853.
30 Lim,F. and Peabody,D.S. (1994) *Nucleic Acids Res.*, **22**, 3748–3752.
31 Spingola,M. and Peabody,D. (1997) *Nucleic Acids Res.*, **25**, 2808–2815.
32 Kraulis,P.J. (1991) *J. Appl. Crystallogr.*, **24**, 946–950.